Particulate Adhesion and Removal from Substrates

THESIS

Presented in Partial Fulfillment of the Requirements for the Honors Research Distinction within the College of Engineering at The Ohio State University

By
Patrick William Beal
Undergraduate Program in Mechanical Engineering

The Ohio State University
2017

Dissertation Committee:
Dr. Carlos Castro – Advisor
Dr. Satya Seetharaman – Co-Advisor
Dr. Jason Dreyer

Abstract

One of the major issues plaguing the semiconductor industry is the adhesion of submicron-sized particles (called particulates) to silicon wafers (substrates) during wafer manufacturing. Such substrate contamination results in unreliable performance of the wafers when used as the foundation for integrated circuits, causing electronic device failure. Currently, brush cleaning, Atomic Force Microscope (AFM) manipulation, and laser induced shock waves are utilized to cleanse contaminated substrates. While these are genuine contributions to particulate removal efforts, the prohibitive cost and lack of efficiency in mass-scaling these techniques pose major issues. This project aims to develop an efficient technique to remove particulates from substrates.

The proposed removal method involved the central premise: vibratory excitation of a substrate may lead to relative motion between the adhering particulate and substrate, thereby breaking the adhesion bonds between the two, leading to particulate removal. To test this claim, a physics-based model was created and microscale and macroscale experiments were carried out to validate the model. During both the microscale and macroscale experimentations, relative motion between a particulate and substrate was observed for a range of frequencies. Although the motion of the particulate was not able to be quantified with respect to time on the microscale, the theoretical model was able to predict the measured aperiodic behavior of the particulate in the macroscale experiments. Oscillating a substrate was ultimately determined to be a plausible methodology to effectively remove particulates from substrates.

It is further expected that future parametric analysis of the microscale model and experiments will aid in the development of a more polished removal method. In doing so, the project's central aim, to establish a prototype to successfully clean contaminated wafers, may be realized, leading to the potential saving of extraneous amounts of physical and financial waste within the semiconductor industry.

Acknowledgments

I would like to express my heartfelt gratitude to Dr. Satya Seetharaman. From this project's conception to its end, Dr. Seetharaman generously gave his time to continually guide me through the ups and downs of this journey. He served as an excellent instructor, passionate about the elegant dynamics of this project. More importantly, he was and continues to serve as a significant role model and mentor. I cannot thank Dr. Seetharaman enough for the invaluable lessons he has taught me during our time together, including but not limited to the importance of patience, personal reflection, and passion for all one does. Dr. Seetharaman continually instilled confidence in me and my abilities. This confidence has helped me throughout this research experience and has propelled me forward during my undergraduate career at Ohio State.

I would also like to thank Dr. Carlos Castro for generously serving as my primary advisor and Dr. Jason Dreyer for his insights while serving on my committee. Their desire to assist students within the Mechanical Engineering Department are very apparent and extremely appreciated.

Without the love and support of my parents, siblings, Emily, Brian, and Ashely, grandparents, and extended family, I would not be the young man I am today. My family has consistently driven me to utilize my time and talents to make a difference in this world. With their help, I am eager to continue to strive to make an impact in my community. I would also like to thank my very special friend who has consistently pushed me to approach

each day with an optimistic and energetic outlook. Thank you for driving me to be my best and for filling each day with bountiful sunshine.

Vita

Aug. 2009 - May 2013 .....Medina Senior High School
Aug. 2013 – May 2017 .....B.S. Mechanical Engineering, The Ohio State University

Fields of Study

Undergraduate Field: Mechanical Engineering

Table of Contents

List of Tables

List of Figures

CHAPTER 1 | INTRODUCTION

1.1 ADHESION OF PARTICULATES TO SUBSTRATES

Within the semiconductor industry, silicon wafers, also known as silicon substrates, are essential in the fabrication of integrated circuits (ICs) [1]. During the manufacturing process, a boule of silicon is sliced into thin (200-300 μm tk.) wafers. The cut wafers are then polished and chemically cleaned in an attempt to remove particulates and other contaminants. After the removal of the contaminants, the wafers serve as the scaffolds upon which ICs are constructed. These ICs are essential components in electronic devices, such as computers and microprocessors [2-3]. However, micro/nano-sized residual silicon burr and silt particulates that adhere to the wafer due to intermolecular adhesive forces may survive the polishing and chemical cleaning. These residual particulates cause uncontrolled variations in the performance of ICs built upon contaminated wafers, leading to unforeseen variations and failure in electronic devices [4].

The unwanted adhesion of particulates to substrates and surfaces also raise challenges in other industries, such as the medical industry. For instance, surface-associated bacterial attachment and growth can take place due to adhesion. This results in the accretion of biological matter on surfaces, known as biofouling. Pathogenic bacteria that adhere to medical devices develop structured communities of microbial cells on the device's surface, leading to disease, and in severe cases, mortality [5].

Although unwanted particulate adhesion to substrates may be detrimental in a number of industries, this research project focused on the adhesion of residual burr and silt particulates to silicon substrates within the semiconductor industry.

1.2 ADHESION AND GRAVITATIONAL FORCES

The primary forces acting on a general particulate adhering to the surface of a substrate are Electrostatic, Capillary, van der Waal (VDW), and Gravitational forces [6]. The relationship between these forces for varying particulate sizes is shown in Figure 1.

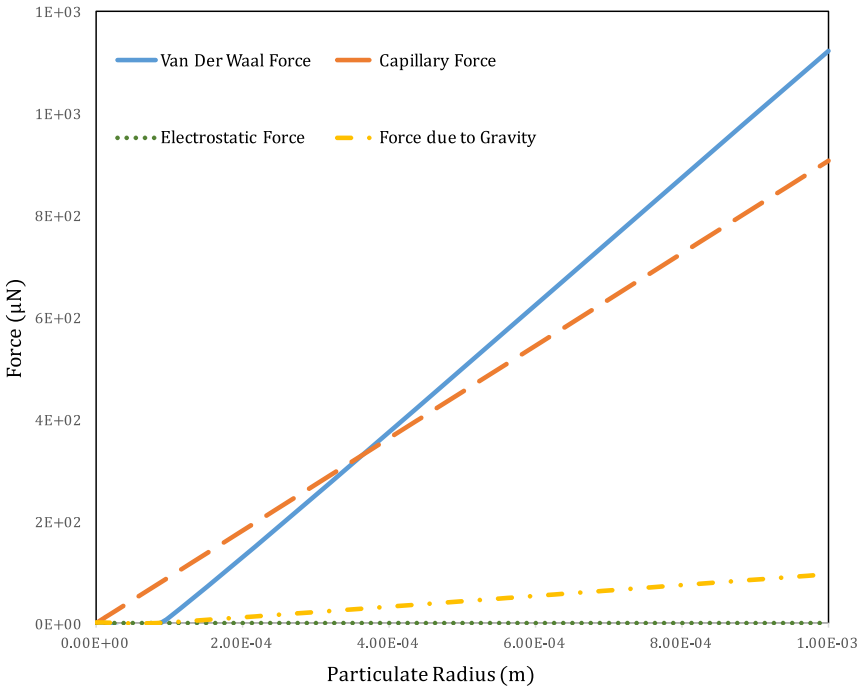

Figure 1: Adhesion and gravitational forces acting on various size particulates adhering to substrates.

1.2.1 ELECTROSTATIC FORCES

Electrostatic forces, or Coulomb forces, involve the attraction or repulsion of particulates and substrates based on their electrical charges. The electrostatic force can be calculated using Equation 1:

$$F_{ELEC} = \frac{\pi \sum RU^2}{l} \quad (1)$$

where *R* is the radius of the particulate, *U* is the potential in volts, and *l* is the separation distance between the particulate and substrate [6].

Nevertheless, as shown in Figure 1, the Electrostatic forces present between a micro-size particulate and a substrate when separated by 1 nm, a plausible surface roughness between a particulate and substrate, is negligible in comparison to Capillary, VDW, and Gravitational forces. Therefore, the Electrostatic forces present between a particulate and a substrate may be discounted.

1.2.2 CAPILLARY FORCES

At relatively high humidity, liquid between a particulate and substrate can create a bonding bridge. This bonding bridge strengthens the adhesion between the particulate and the substrate, resulting in a Capillary force [7]. The Capillary force, which heavily relies on the particulates size and the surface tension of the present fluid, can be calculated using Equation 2:

$$F_{CAP} = \frac{4\pi\gamma R cos\theta}{(1 + \frac{x}{x_o})} \quad (2)$$

where γ is the surface tension of the present fluid, θ is the contact angle between the particulate and the substrate, x is the distance between the particulate and substrate from the bottom end of the particulate, and x_o is the distance between the meniscus of the fluid layer and the bottom of the particulate [6].

Nevertheless, Capillary forces do not constitute a dominant particulate adhesion force in relative humidity lower than 70 percent. The relative humidity in a semiconductor clean room is typically controlled to a target value within 30 to 50 percent humidity, held with tolerances as low as +/- 1 percent. Therefore, the Capillary force can be deemed negligible for the purposes of this project [7].

1.2.3 VAN DER WAAL (VDW) FORCES

Even if a particulate and substrate are neutral in charge, these objects are polarized due to fluctuation in their electron clouds. This results in a short-range adhesion force between the particulate and the substrate, known as the van der Waals force. Equation 3 is utilized to compute this VDW force:

$$F_{VDW} = \frac{AR}{6l^2} \tag{3}$$

where A is the Hamaker constant, R is the particulate's radius, and l is the separation distance between the particulate and the substrate. The Hamaker constant, which reflects the strength of the VDW force and depends on the type of material used for the particulate and the substrate, is given as $A = \pi^2 C \rho_1 \rho_2$, where C is the coefficient in the atom-atom pair potential, and ρ_1 and ρ_2 are the number of atoms per unit volume in the two bodies.

As shown in Figure 1, the VDW serves as a dominant force, causing stiction between silicon particulates and substrates [6,8].

1.2.4 GRAVITATIONAL FORCE

In addition to the VDW adhesion force present between the particulate and the substrate, a Gravitational force is also present. Equation 4 represents the Gravitational force acting on the particulate as it adheres to the substrate:

$$F_{GRAV} = \frac{4\pi R^3 \rho g}{3} \tag{4}$$

where R is the radius of the particulate, ρ is the density of the particulate's material, and g is the gravitational constant. As shown in Figure 1, gravity is the second most prominent force when assuming a negligible Capillary force.

1.2.5 RELATIONSHIP BETWEEN VDW AND GRAVITATIONAL FORCES

As a result of negligible Electrostatic and Capillary forces between silicon particulates and substrates within the semiconductor industry, VDW and Gravitational forces are the dominant forces acting between a silicon particulate and a silicon wafer. The relationship between VDW and Gravitational forces and the separation distance between a particulate with a 10μm radius and substrate is show in Figure 2.

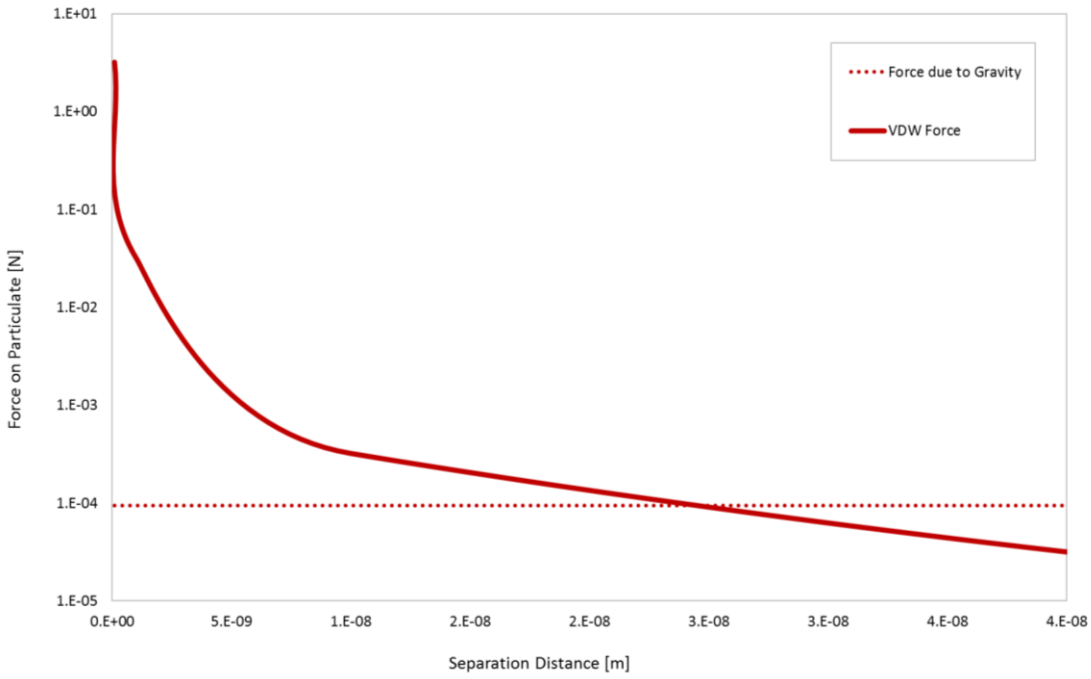

Figure 2: VDW and Gravitational forces on particulate with respect to separation distance between particulate and substrate.

The Gravitation force is independent of the separation distance between the particulate and the substrate. The VDW Force, on the other hand, is inversely proportional to the separation distance between the particulate and the substrate. Therefore, particulate removal has a higher chance of success if the separation distance between a particulate and a substrate increases.

1.3 CURRENT REMOVAL METHODS

Several particulate removal techniques have been developed to address contamination of substrates. The common removal methodologies utilized within the semiconductor and

other industries are brush cleaning, manipulation via an Atomic Force Microscope (AFM), and laser induced shock waves [2, 9-11].

One of the most common and prevalent removal methods was developed by Busnaina et al. in 2002. This method, shown in Figure 3a, utilizes a brush to sweep across the top of a contaminated substrate. By adjusting the brush rotational speed and brush pressure applied to the substrate, this technique aims to increase the separation distance between the particulates and substrate, thereby weakening the present VDW force. With a weakened adhesion force, a flow of water or air is sent across the substrate inducing a drag force, which rolls or slides the particulate off the surface of the substrate [2].

Manipulation via an AFM and laser induced shock waves are also utilized to remove unwanted particulates from substrates. Using an AFM to remove particulates involves utilizing the AFM tip to manipulate a single particulate, displace it from its initial position on the substrate, and remove it from the substrate's surface [9-10]. The use of laser induced shock waves, on the other hand, involves sending a shock wave across the top of a substrate and exciting particulates off the substrate's surface [11]. Schematics of AFM manipulation and the use of laser induced shock waves are shown in Figure 3b and 3c, respectively.

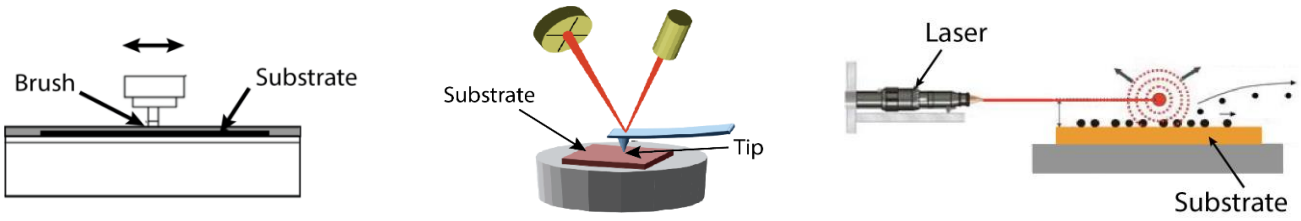

a b) c)

Figure 3: a) Brush cleaning technique b) AFM manipulation c) laser induced shock waves.

While these three removal methodologies are genuine contributions to particulate removal efforts, the wear of brush cleaning, the lack of efficiency in mass-scaling of AFM manipulation, and the prohibitive cost of laser induce shock waves pose major issues in the cleaning of substrates.

1.4 PURPOSE AND OBJECTIVES OF RESEARCH

The purpose of this research project is to develop an efficient technique to remove particulates from substrates.

The objectives of this project are as follows:

1) Derive and model a method to remove particulates from substrates.
2) Design and conduct experiments to validate the theoretical model.
3) Draw conclusions on the potential of the proposed removal method.

1.6 PROPOSED REMOVAL METHOD AND HYPOTHESIS

The proposed removal method aims to increase the separation distance between an adhering particulate and a substrate by oscillating the substrate with sufficient amplitudes and frequencies.

In oscillating the substrate, the particulate is predicted to move relative to the substrate. This relative motion is desired because it will result in a separation distance between the particulate and the substrate. This separation distance will diminish the VDW force acting on the particulate and provide ample opportunities for particulate removal by means of an external source, such as a water or air stream.

CHAPTER 2 | REMOVAL BY OSCILLATION – MODEL

2.1 INTRODUCTION

This chapter focuses on the development of a physics-based model of the proposed, oscillatory removal methodology. The first part of this chapter outlines the assumptions made during the formulation of this model. This is followed by the analysis completed to derive the equations of motion of the particulate during multiple stages of its interaction with the substrate, including adhesion to the substrate, initial separation from the substrate, and induced independent motion following separation.

2.2 ASSUMPTIONS

1. The interaction between a spherical particulate and a flat substrate surfaces is considered while formulating the system dynamics.
2. As mentioned in the previous chapter, Electrostatic and Capillary forces between the particulate and the substrate are neglected. The major forces contributing to stiction are the VDW and Gravitational forces.
3. When the separation between the particulate and the substrate is larger than the surface roughness, 1 nm, the VDW force breaks down and the only force acting on the particulate is the force due to gravity.
4. All motion is assumed to occur in the two dimensional space, and the particulate is represented as a point mass rather than a three dimensional rigid body.

2.3 SYSTEM DYNAMICS

The system dynamics of the proposed removal methodology is separated into four stages. The first stage comprises of a particulate adhering to the surface of an oscillating substrate. In this step, the particulate and the substrate move together as one. The second stage involves discovering the time at which the particulate is removed from the oscillating substrate. In step three, the particulate moves independent of the substrate, and in step four, the particulate collides with the oscillating substrate. Steps three and four are then continuously repeated. The equations of motion of these four steps were implemented into MATLAB, the program utilized to run the theoretical model [12]. The model's MATLAB code is shown in Appendix A.

2.3.1 PARTICULATE ADHERES TO SUBSTRATE

The first stage in modelling the behavior of a particulate adhering to an oscillating substrate involves stiction between the particulate and the substrate. This stiction, due to the present VDW and Gravitational forces, causes the particulate and the substrate to move as one, shown in Figure 4. The mass of the particulate is denoted as m, and the mass of the substrate is denoted as M. Likewise, the positions of the particulate and the substrate are denoted as y_p and y_s, respectively. The substrate undergoes simple harmonic motion, exemplified in Equation 5. Since the particulate and the substrate act as one body, the acceleration, shown in Equation 6, are the same for both objects. In Equations 5 and 6, δ is the amplitude of oscillation, ω is the frequency of oscillation, and t is time.

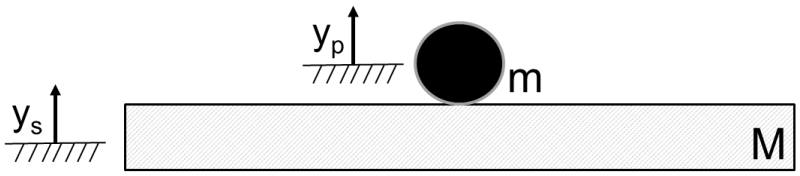

Figure 4: Schematic of particulate adhering to substrate.

$$y_s = y_p = \delta sin(\omega t) \tag{5}$$

$$\ddot{y_p} = -\delta\omega^2 \sin(\omega t) \tag{6}$$

2.3.2 PARTICULATE LOSES CONTACT WITH SUBSTRATE

The second stage of the theoretical model focuses on the moment at which the particulate loses contact with the substrate. The free body and kinetic diagrams depicting this event are shown in Figure 5.

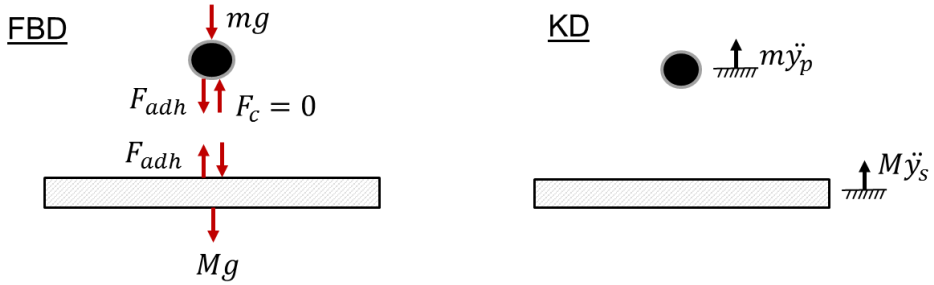

a) b)

Figure 5: a) Free body and b) kinetic diagram of the system when the particulate loses contact with the substrate.

As previously mentioned, the present adhesion force, F_{adh}, is equal to the VDW force on the particulate. Moreover, since the particulate is losing contact with the substrate

in this step, the contact force, depicted as F_c, is set to 0 N. By performing a force balance on the two diagrams shown in Figure 5, the time at which the particulate loses contact with the substrate can be derived by using Equations 7-9:

$$-\frac{F_{adh}}{m} - g = \ddot{y_p} \tag{7}$$

$$-\frac{F_{adh}}{m} - g = -\delta\omega^2 \sin(\omega t_{loss}) \tag{8}$$

$$t_{loss} = \sin^{-1}\left\{\frac{g + \frac{F_{adh}}{m}}{\delta\omega^2}\right\}\frac{1}{\omega} \tag{9}$$

where g is the gravitational constant and t_{loss} is the time at which the particulate loses contact with the substrate.

It is important to determine the time at which the particulate loses contact with the substrate because the time can be utilized in the MATLAB program to find the position and the velocity of the particulate when loss of contact occurs. These values serve as initial conditions for the motion of the particulate outlined in step three.

2.3.3 PARTICULATE MOVES INDEPENDENT OF SUBSTRATE

After the particulate initially loses contact with the substrate, it begins to move independent of the substrate. As mentioned in the assumptions, once the particulate and the substrate are separated by the surface roughness of the substrate, 1 nm, the adhesion force significantly diminishes and the only force acting on the particulate is the force due to gravity. Therefore, after losing contact with the substrate, the particulate experiences projectile motion, independent of the motion of the substrate. The free body and kinetic diagram of the particulate as it undergoes projectile motion is shown in Figure 6.

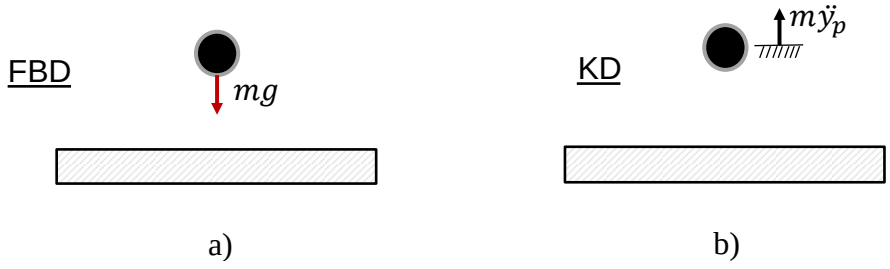

Figure 6: a) Free body diagram and b) kinetic diagram of the particulate as it moves independent of the substrate following loss of contact.

By performing a force balance on the particulate's free body and kinetic diagrams, the particulate's equation of motion can be derived. The particulate's equation of motion for this step of the model is shown as Equation 10.

$$\ddot{y}_p = -g \tag{10}$$

2.3.4 PARTICULATE COLLIDES WITH SUBSTRATE

The final step in the theoretical model of a particulate on an oscillating substrate involves a collision between the particulate and the substrate. As the particulate undergoes projectile motion after losing contact with the substrate, the force due to gravity brings the particulate back into contact with the substrate. This occurrence can be treated as a collision event, shown in Figure 7.

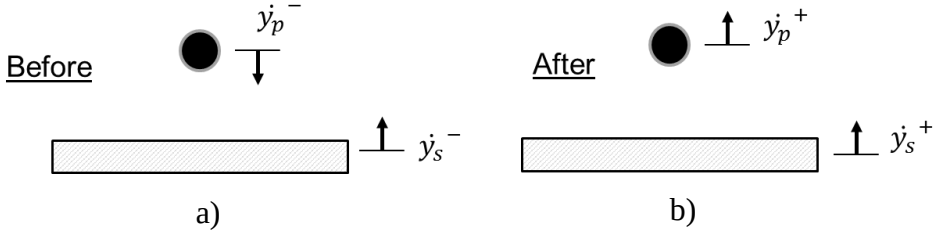

Figure 7: Schematic of the particulate and substrate a) before the collision event and b) after the collision event.

Since this step is treated as a collision event, the particulate's coefficient of restitution, *e*, can be utilized to determine the velocity of the particulate after the collision. The relationship between the coefficient of restitution and the velocities of the particulate and substrate before and after the collision is outlined in Equation 11.

$$e = \frac{\dot{y_s}^+ - \dot{y_p}^+}{-\dot{y_p}^- - \dot{y_s}^-} \tag{11}$$

In this equation, the velocity of the particulate before the collision, $\dot{y_p}^-$, the velocity of the substrate before the collision, $\dot{y_s}^-$, and the velocity of the substrate after the collision, $\dot{y_s}^+$, are known at the time of the collision event. Using Equation 11 and its known values, the velocity of the particulate following the collision event, $\dot{y_p}^+$, can be determined. The velocity and position of the particulate after the collision can be used as initial conditions as the particulate returns to projectile motion. The projectile motion of the particulate and the collision of the particulate and substrate are continually repeated.

CHAPTER 3 | REMOVAL BY OSCILLATION – EXPERIMENTATION

3.1 INTRODUCTION

Following the development of the model, experiments were designed and conducted in order to validate the theoretical model. Due to the nature and scale of the problem in the semiconductor industry, microscale experimentations were initially completed. However, due to lack of proper measuring equipment, the motion of the particulate could not be sufficiently tracked. As a result, macroscale experiments were designed. On the macroscale, the motion of the particulate was tracked and compared to the motion of the particulate within the developed model. The following sections within this chapter outline the setup, parameters, and procedures of the microscale and macroscale experiments.

3.2 MICROSCALE EXPERIMENTATION

The first experimentations for this project were completed on the microscale in order to simulate the scale of a particulate on a substrate within the semiconductor industry. For these experiments, a discrete, 150V, 20 μm free stroke piezo stack's top served as the substrate. When a voltage was driven into the piezo stack, it underwent uniform oscillatory motion. The voltage was delivered to the piezo stack via a power generator and PDu150 piezo driver. The input voltage was inversely proportional to the piezo stack's amplitude and directly proportional to the stack's frequency. Plastic microbeads served as the particulate in these microscale experiments. These microbeads had radius dimensions

ranging from 100um to 3mm and an average mass of 1.90 mg. The coefficient of restitution of the microbead was assumed to be 0.9. The microscale experimental setup is shown in Figure 8 and Figure 9.

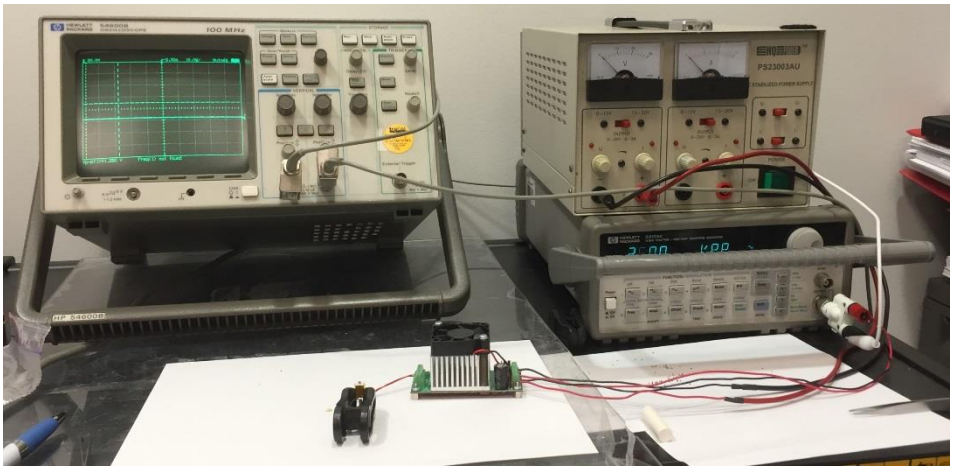

Figure 8: Overall setup of micro-scale experimentation.

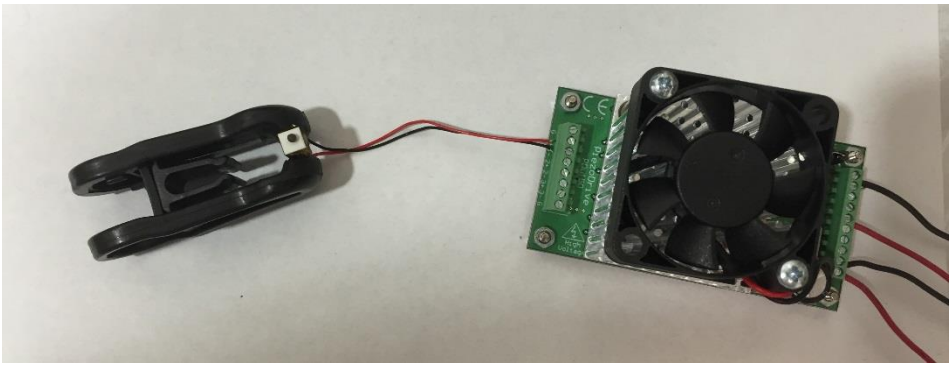

Figure 9: Close up of piezo stack, microbead, and piezo driver.

In order to conduct the experiment, a microbead was positioned on the top of the piezo stack. The piezo stack was then oscillated at various amplitudes and frequencies over the course of 20 tests. Due to the lack of proper equipment, numerical data of the particulate's motion was not able to be collected. The amplitude of the piezo stack was

unable to be collected as well. Nevertheless, the motion of the microbead for the various tests was visually observed and tracked.

Due to the inability to collect numerical data to outline the particulate's response to the oscillation of the substrate, the MATLAB model was unable to be validated. In order to conduct experimentations to verify the model, the possibility of scaling the experimental setup to the macroscale was considered. Within the theoretical model, the only parameters that would be affected by scaling the system would be the radius and mass of the particulate. Since these parameters do not breakdown via scaling, it was determined that scaling the experiment would be a viable option to verify the model. In order to validate this claim, the model was utilized to plot the motion of a particulate oscillating on a substrate on the microscale and macroscale. As shown in Figure 10, the behavior of the particulate in both the microscale and macroscale was aperiodic in nature, revealing that the physics of the system was similar on both the microscale and macroscale. This finding further validating the scaling of the experimental setup.

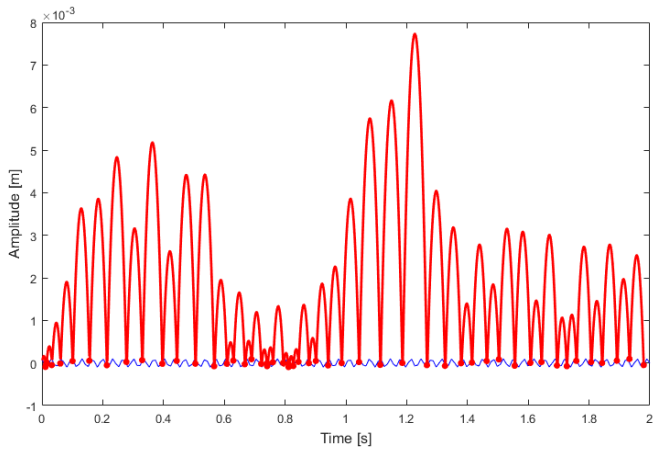

Particulate Mass: 0.017 mg
Particulate Radius: 0.1 mm
Frequency: 70 Hz
Amplitude: 0.1 mm

a)

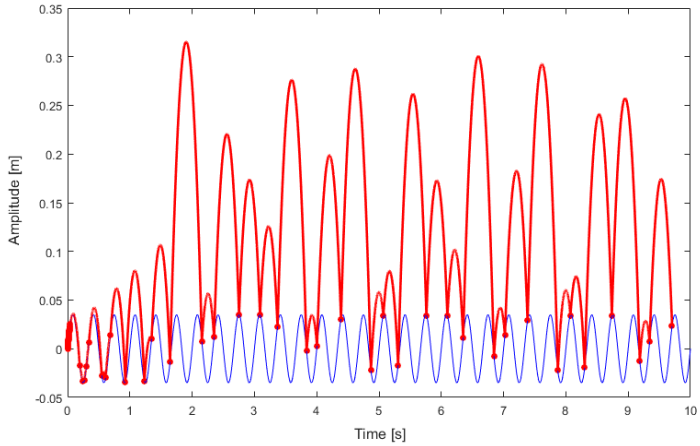

Particulate Mass: 2.7 g
Particulate Radius: 20 mm
Frequency: 3 Hz
Amplitude: 35 mm

b)

Figure 10: a) microscale simulation b) macroscale simulation**.**

3.3 MACROSCALE EXPERIMENTATION

In order to validate the theoretical model following the inability to do so with the microscale experiments, a macroscale experimental setup was developed. This setup included a PVC tube, wooden piston, and AC motor. The piston, attached to a shaft, was driven by the motor and translated within the PVC tube. The head of the piston served as the substrate within this experimental setup. The amplitude of the substrate's oscillation was determined by the length of the connecting shaft, which was 35 mm. The substrate's frequency was varied by alternating the radial speed of the motor. A ping-pong ball was utilized as the particulate in this setup's experimentation. The mass of the ping-pong ball was 2.7 g and its radius was 20 mm. The coefficient of restitution of the ping-pong ball was 0.9. The setup for the conducted macroscale experiments is shown in Figure 11.

Figure 11: Setup of macroscale experimentations.

In order to conduct the experiments, the ping-pong ball was placed in the PVC tube. The piston was then oscillated at various frequencies for four tests. The four tested frequencies were 2, 3, 4, and 5 Hz. The behavior of the oscillating ping-pong ball was captured on video for each test and the video was uploaded to Tracker 4.95, a video analysis software [13]. Tracker 4.95 was able to follow the motion of the ping-pong ball and plot the ball's motion. Using the parameters from the macroscale experiments, the outcomes of the MATLAB model were compared to the experimental motion data of the ping-pong ball for each tested frequency.

CHAPTER 4 | RESULTS AND CONCLUSIONS

4.1 INTRODUCTION

This chapter includes the results and conclusions derived from the performed experiment and theoretical model. The first section of this chapter outlines the envelop of voltages and frequencies in which motion of the particulate in the microscale experiments was visually observed. The second section outlines the experimental findings from the macroscale experiments and the comparison between the macroscale results and the theoretical model. The final section discusses the proposed future work needed to continually research and develop the proposed removal method.

4.2 RESULTS FROM MICROSCALE

As mentioned in the previous chapter, due to the lack of proper equipment, the particulate's motion with respect to time was unable to be quantified. Likewise, the amplitude of the piezo stack was unable to be collected. Nevertheless, results from tests in which the piezo stack's frequency and input voltage were altered revealed an envelope in which relative motion between the particulate and substrate was visually observed. This envelop of voltages and frequencies that resulted in particulate motion is shown in Figure 12.

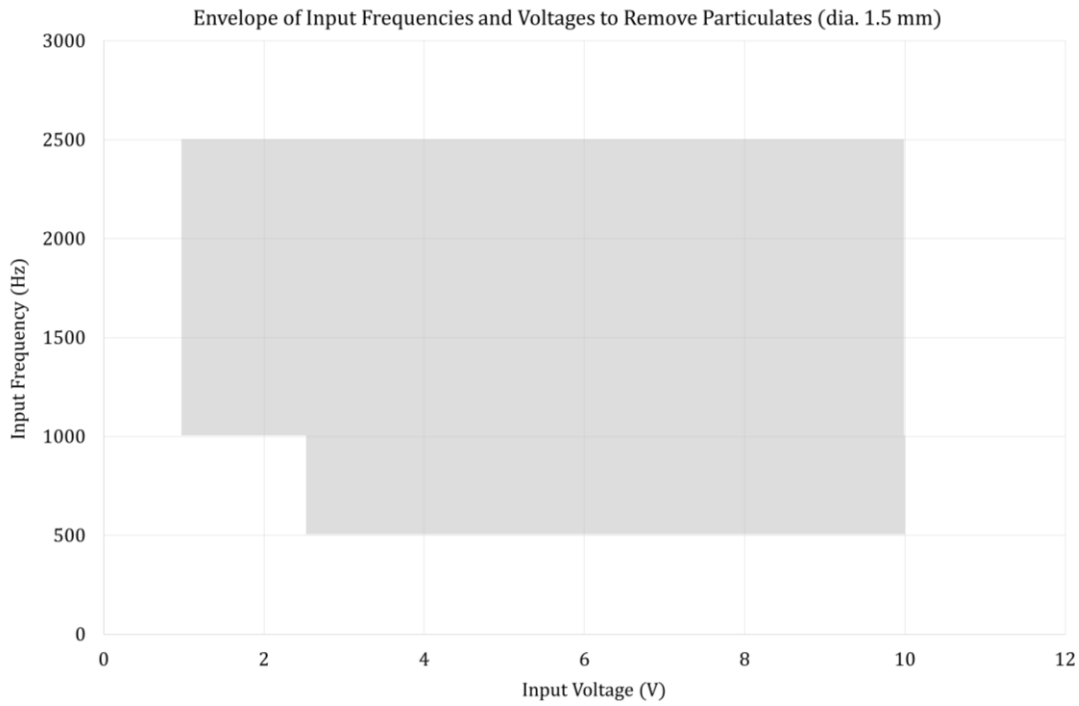

Figure 12: Envelope of input voltages and piezo stack frequencies in which particulate motion was visually observed.

As shown in Figure 12, motion of the particulate was visually observed for various combinations of input voltage-dependent amplitudes and frequencies. However, due to the inability to track the amplitude of the substrate's oscillation, conclusions were unable to be drawn on the effectiveness of inducing separation between a particulate and substrate for specific frequency and oscillation amplitudes.

Due to the inability to collect numerical data to outline the particulate's response to the oscillation of the substrate, the accuracy of the physics-based model was unable to be validated. Nevertheless, the macroscale experimental setup was created to quantify the motion of a particulate on an oscillating substrate and verify the system dynamics of the model.

4.3 RESULTS FROM MACROSCALE

Unlike the microscale experiments, the macroscale experiments were able to quantify the motion of the particulate with respect to time. Using the macroscale experimental setup, four different tests were conducted using oscillatory substrate frequencies of 2, 3, 4, and 5 Hz. The motion of the particulate for these tests are shown in Figures 13-16.

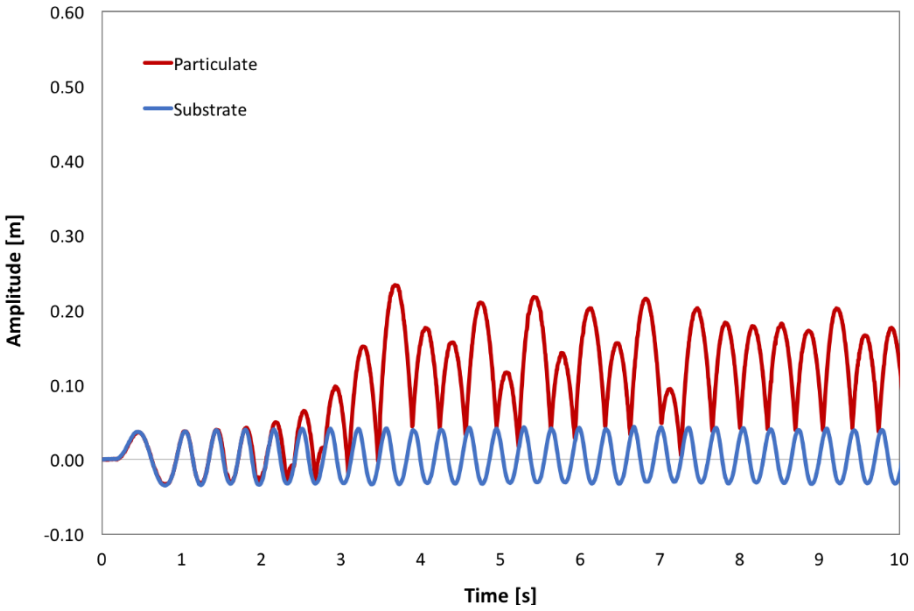

Figure 13: Experimental motion of particulate when substrate oscillated at 2 Hz.

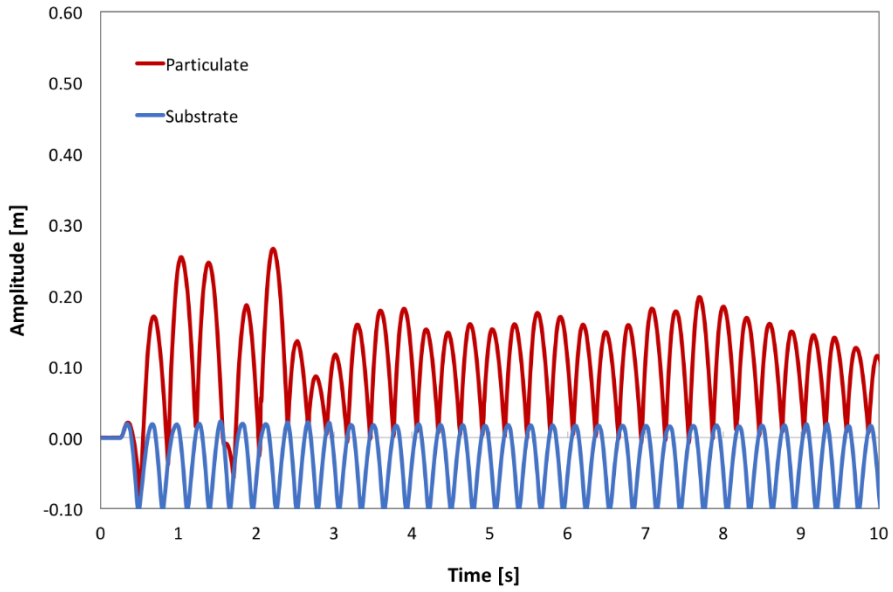

Figure 14: Experimental motion of particulate when substrate oscillated at 3 Hz.

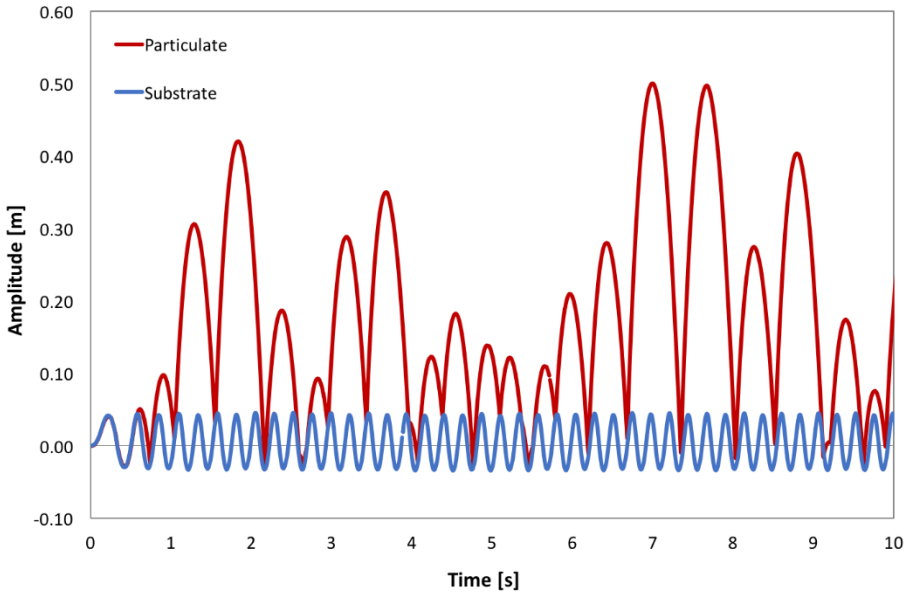

Figure 15: Experimental motion of particulate when substrate oscillated at 4 Hz.

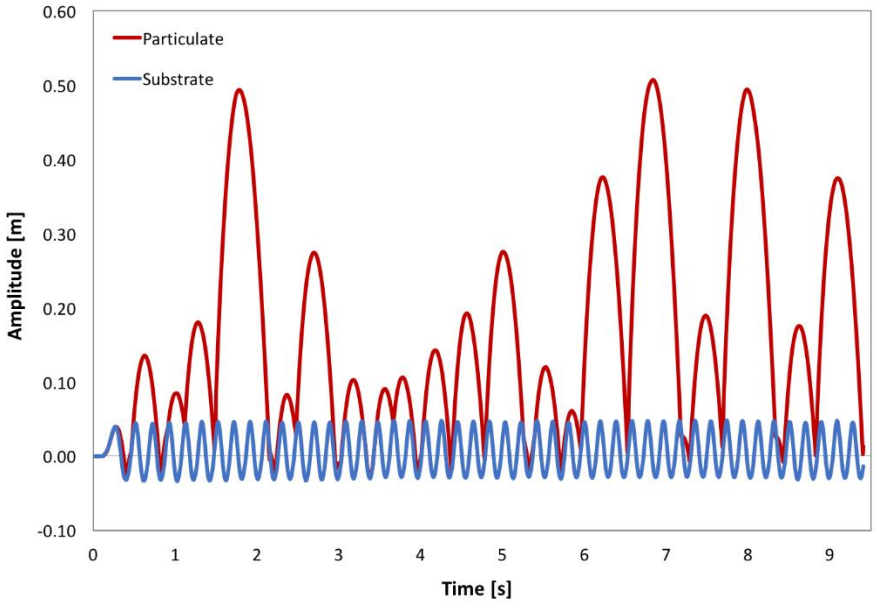

Figure 16: Experimental motion of particulate when substrate oscillated at 5 Hz.

The motion of the particulate when the substrate was oscillated at 2 Hz and 3 Hz was more uniform in motion than when the substrate was oscillated at 4 Hz and 5 Hz. The motion of particulate for both the 4 Hz and 5 Hz case, as shown in Figure 15 and Figure 16, was aperiodic in nature. These two test cases also resulted in the largest separation distances between the particulate and the substrate. The maximum separation distances for these four tests are shown in Table 1.

Table 1: Maximum amplitudes of the particulates for each tested substrate frequency.

Frequency of Substrate's Oscillation [Hz]	Maximum Amplitude of Particulate [m]
2	0.233
3	0.266
4	0.500
5	0.507

Unlike the microscale experiments, data collected from the macroscale experiments were able to be compared to the theoretical model. Since the largest separation distances between the particulate and the substrate occurred while the substrate oscillated at 4 Hz and 5 Hz, the experimental motion of the particulate for these tests were compared to the particulate's motion from the model. In order to properly model these two tests, the parameters of the experimental particulate and the frequency of the substrate were entered into the model's MATLAB code. The comparisons between the experiments and theoretical model for these tests are shown in Figure 17 and Figure 18.

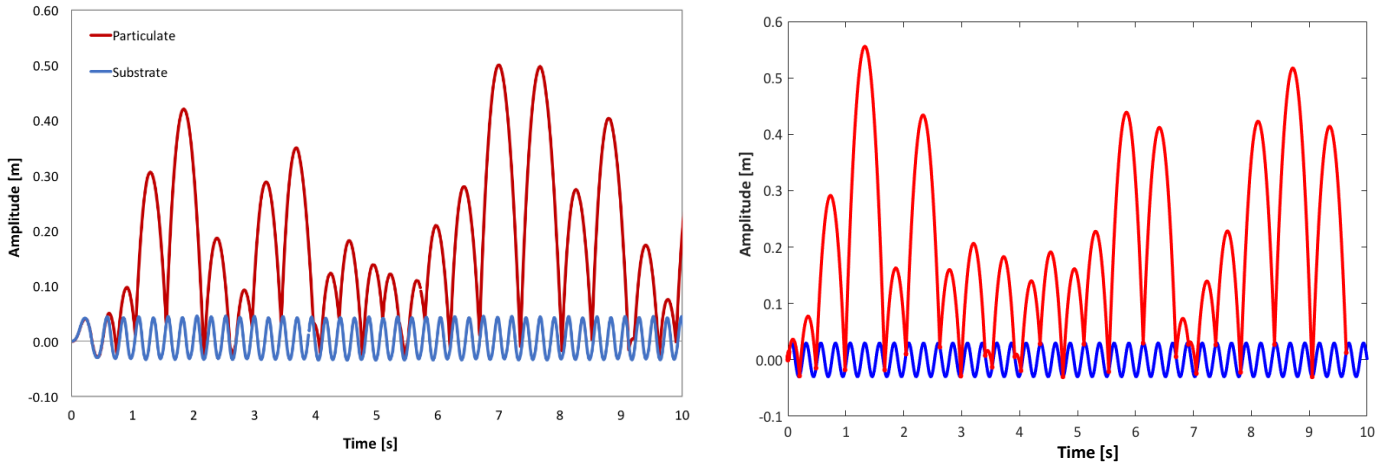

a) b)

Figure 18: The a) experimental and b) theoretical motion of a particulate on a substrate oscillating at 4 Hz.

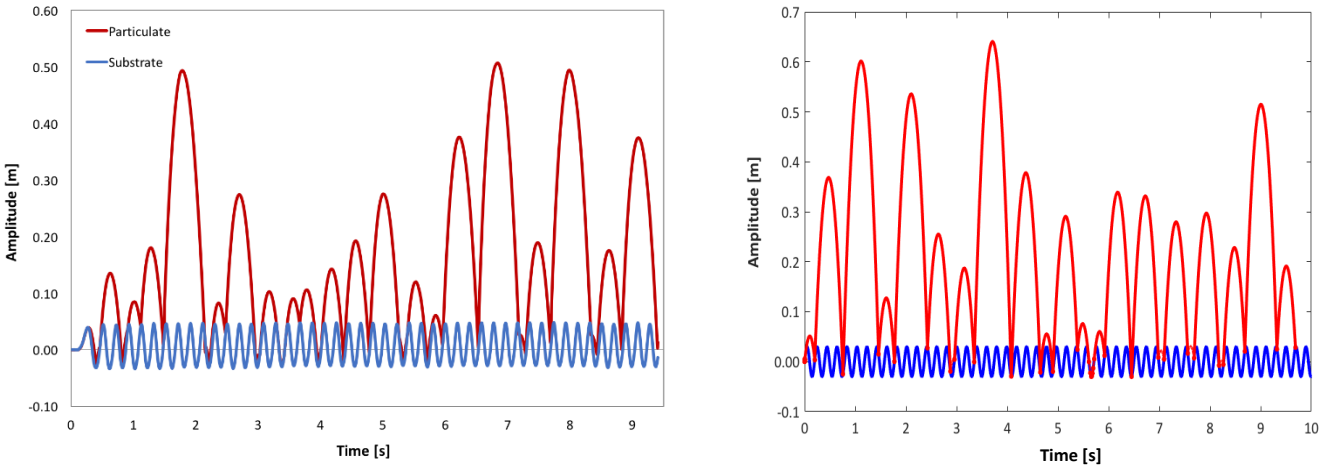

a) b)

Figure 19: The a) experimental and b) theoretical motion of a particulate on a substrate oscillating at 5 Hz.

The motion of the particulate for both the 4 Hz and 5 Hz experiments and the model, at these respective frequencies, was aperiodic. Furthermore, the maximum amplitudes of the model when the substrate was oscillated at 4 Hz and 5 Hz were 0.556 m and 0.640 m, respectively. These theoretical maximum amplitudes were slightly larger than the experimental amplitudes observed in both tests. However, this was expected, as the model depicted the system in two dimensions, yet the experiment was conducted in three dimensions. Therefore, the model did not account for the rigid body rotation of the particulate nor the forces due to drag that are present within the experimental setup.

Overall, the aperiodic behavior of the particulate and the similar amplitudes of the particulate in both the experimental data and the model provided substantial evidence that the physics-based model was representative of a particulate's behavior on an oscillating

substrate. As a result, the model could be utilized to draw conclusions about a particulate's behavior in both the macroscale and microscale, assuming the same dominating physics for both scales.

4.4 FUTURE WORK

Although the model was proven to be representative of a particulate's behavior on an oscillating substrate, continued investigation can be completed to sufficiently cover the basis of this proposed removal methodology. The following is a list of future work that may be completed:

- Perform a parametric analysis on the microscale with the current model in order to determine the optimal theoretical frequencies and amplitudes that would lead to particulate removal.
- Obtain equipment needed to perform microscale experiments and execute experiments to test the proposed methodology on the scale of the problem within the semiconductor industry.
- Investigate a mesh collection device to remove the particulate once separated from the substrate and design methodology to fit within the manufacturing process.
- Perform failure analysis on the oscillating silicon substrate to ensure the substrate is not damaged due to the induced oscillations.
- Explore, model, and conduct experiments in the case when multiple particulates are adhering to a single substrate.

- Investigate the stability of the system by deriving the Lyapunov and investigating period doubling to mathematically determine if the particulate's aperiodic motion is indicative of a chaotic system.

BIBLIOGRAPHY

1. *Laplante, P., "Comprehensive dictionary of electrical engineering", CRC Press., 2005.*
2. Zhang, F., Busnaina, A., Ahmadi, G., "Particle Adhesion and Removal in Chemical Mechanical Polishing (CMP) and post-CMP Cleaning", Journal of The Electrochemical Society, 1999.
3. "*Basic Integrated Circuit Manufacturing*", Integrated Circuit Engineering Corporation.
4. Uemura, K., Haibara T., Mori Y., "*Cleaning Technology of Silicon Wafers*", Nippon Steel Technical Report, No. 83, 2001.
5. Graham M.V., Cady N.C., "*Nano and Microscale Topographies for the Prevention of Bacterial Surface Fouling*", 2014.
6. Seetharaman, Satya. MS Thesis. Iowa State University. 2004.
7. Donovan, Robert P. "Why Control Humidity in a Cleanroom?" *Solid State Technology – Insights for Electronics Manufacturing*. Extension Media, n.d. Web.
8. Hattori, Takeshi. *Ultraclean Surface Processing of Silicon Wafers: Secrets of VLSI Manufacturing*. Berlin: Springer, 1998. Print.
9. Sitti, M., "*Teleoperated and automatic control of nanomanipulation systems using atomic force microscope probes*", Conference on Decision and Control, 2003.

10. Junno, T., Deppert, K., Montelius, L., Samuelson, L., "*Controlled Manipulation of Nanoparticles with an Atomic Force Microscope*", Applied Physics Letter 66, American Institute of Physics, 1995.
11. Curran, C., Watkins, K.G., Lee, J.M., "*Shock Pressure Measurements for the Removal of Particles on Sub-micron Dimensions from Silicon Wafers*", 21st International Congress on Applications of Lasers and Electro-Optics, 2002.
12. "*MATLAB*" © Mathworks, 2015.
13. "*Tracker 4.95*" © Open Source Physics.

Appendix A: MATLAB PROGRAM

```
function particulate_chaos

clc
clf
clear all
close all

% Set parameters
eV = 1.602e-19;
A = (3/4/pi)*6.76*eV;
r_p = 0.75e-3;
g = 9.8;
rho = 4000;
m = rho*(4/3)*pi*r_particle^3;
del = 2e-3;
omega = 2*pi*1.5;
mu_roughness = 1e-9;

% Set end time and number of data points
t_end = 15;
n = 1000;
tspan = linspace(0,t_end,n);
N = zeros(length(n));

% First time at which particulate loses contact
t_loss = (1/omega)*asin((m_p*g)/(m_p*del*omega^2) + (A*r_p/6/mu_roughness^2)/(m_p*del*omega^2));
y_0 = mu_roughness + del*(sin(omega*t_loss));
y_0dot = omega*del*cos(omega*t_loss);

% set this as equal to t_loss
t_start = t_loss;
t_match = t_loss;
tspan_compare = linspace(t_loss,t_end,n);
y_particulate = y_0;

y_subst =  del*sin(omega*linspace(0,t_end,n));
tspan_compare(1) = t_loss;
```

-
-
-

```
% Using intersection
e_res = 0.9;
t_loss = 0;
t_start_intersection = t_loss;
tspan_compare_intersection = linspace(t_start_intersection,t_end,n);
y_0_intersection = mu_roughness + del*(sin(omega*t_start_intersection(1)));
y_0dot_intersection = omega*del*cos(omega*t_start_intersection(1));
y_dot_substrate_minus = del*omega;
y_dot_substrate_plus = y_dot_substrate_minus;
y_dot_particulate_minus = y_dot_substrate_minus;
y_dot_particulate_plus = y_dot_substrate_plus;
y_particulate_intersection = y_0 + y_0dot*(tspan_compare_intersection-t_start_intersection) - 0.5*g*(tspan_compare_intersection-t_start_intersection).^2;
        for j = 1:((n/2)-1)
        omega = omega_loop(1);
        y_substrate_intersection(j)  = del*sin(omega*tspan_compare_intersection(j));
        end
        for j = (((n/2)+ 1):n)
        omega = omega_loop(2);
        y_substrate_intersection(j) = del*sin(omega*tspan_compare_intersection(j));
        end
        for j = n/2
            y_substrate_intersection(j)  = del*sin(omega*tspan_compare_intersection(j));
        end
plot(tspan_compare_intersection,y_substrate_intersection,'linewidth',2)
hold on
for i = 2:n
    if (i < (n/2))
        omega = omega_loop(1);
    else
        omega = omega_loop(2);
    end
    t_match_intersection = InterX([tspan_compare_intersection;y_particulate_intersection],[tspan_compare_intersection;y_substrate_intersection]);
    t_start_intersection(i) = t_match_intersection(1,1) + t_loss;
    tspan_compare_intersection = linspace(t_start_intersection(i),t_end,n);
    tspan_match_intersection = linspace(t_start_intersection(i-1),t_match_intersection(1,1),n);
    y_particulate_intersection_plot = y_0_intersection + y_dot_particulate_plus*(tspan_match_intersection-t_start_intersection(i-1)) - 0.5*g*(tspan_match_intersection-t_start_intersection(i-1)).^2;
    plot(tspan_match_intersection,y_particulate_intersection_plot,'linewidth',2)
    hold on
    plot(t_match_intersection(1,1),t_match_intersection(2,1),'r.','markersize',18)
    hold on
    y_0_intersection = mu_roughness + del*(sin(omega*t_start_intersection(i)));
    y_dot_substrate_minus = omega*del*cos(omega*(t_start_intersection(i) - 2*t_loss));
    y_dot_substrate_plus = y_dot_substrate_minus;
    y_dot_particulate_minus = y_dot_particulate_plus - g*(t_start_intersection(i) - t_start_intersection(i-1));
    y_dot_particulate_plus = y_dot_substrate_plus - e_res*(y_dot_particulate_minus - y_dot_substrate_minus);
    y_particulate_intersection = y_0_intersection + y_dot_particulate_plus*(tspan_compare_intersection-t_start_intersection(i)) - 0.5*g*(tspan_compare_intersection-t_start_intersection(i)).^2;
    y_substrate_intersection  = del*sin(omega*tspan_compare_intersection);

end

end
```